State-space seismic cone minimum variance deconvolution

Erick Baziw
Baziw Consulting Engineers Ltd., Vancouver, Canada

Keywords: Seismic cone penetration testing (SCPT), minimum variance, Kalman filter, smoothing, autoregressive moving average (ARMA)

ABSTRACT: Seismic Cone Penetration Testing (SCPT) is a geotechnical tool which facilitates the determination of low strain ($<10^{-4}$%) in-situ compression (P) and shear (S) wave velocities. The P-wave and S-wave velocities are directly related to the soil elastic constants of Poisson's ratio, shear modulus, bulk modulus, and Young's modulus. The seismic cone records the arrival of seismic waves generated at the surface using velocity or acceleration transducers installed in an electric piezocone. The in-situ P-wave and S-wave interval velocities are determined by firstly obtaining the corresponding time series arrival times or relative arrival times as the probe is advanced into the soil profile. Inversion analysis is then carried on the recorded P-wave and S-wave arrival times so that corresponding interval velocity profiles are obtained.

In SCPT there are site conditions which result in source wavelet multiples. These multiples complicate the recorded time series making the selection of interval arrival times a difficult task. This paper outlines a state-space smoothing Kalman Filter algorithm which deconvolves impedance structures from recorded source wavelet multiples. It is also demonstrated that the outlined algorithm is a highly beneficial tool in automating the determination of source wavelet arrival times when only a primary wavelet is recorded.

1 INTRODUCTION

There is considerable interest in methods of geotechnical *in-situ* engineering which enable shear (S) and compression (P) wave velocities in the ground to be accurately estimated. These measurements provide insight into the response of soil to imposed loads such as buildings, heavy equipment, earthquakes, and explosions. The S-wave and P-wave velocities are desired because they form the core of mathematical theorems which describe the elasticity/plasticity of soils and are used to predict settlement, liquefaction, and failure (Finn (1984); Andrus et al. (1999)). As such, accuracy in the estimation of shear and compression waves velocities is of paramount importance because these values are squared during the calculation of geotechnical parameters such as the Shear Modulus, Poisson's Ratio, and Young's Modulus, among others.

The Seismic Cone Penetration Test (SCPT) (an extension of the Cone Penetration Test (CPT)) was devised to measure seismic velocities directly through data obtained by installed seismic sensors in the cone penetrometer, in addition to the standard bearing pressure, sleeve friction, and pore pressure sensors (Campanella et al. 1986). As the cone penetrometer is advanced through the ground, using a pushing force, the advance is halted at one meter (or other such increment) intervals. When the cone is at rest, a seismic event is generated at the surface using a hammer blow or explosive charge, causing seismic waves to propagate from the surface through the soil to be detected by seismic sensors installed in the cone penetrometer. This event is recorded and the penetrometer is advanced another increment and the process is repeated. By determining the seismic arrival times interval seismic velocities are calculated over the depth increment under study (Baziw (1993 and 2002)).

In SCPT there are site conditions which may result in source wavelet multiples. These multiples complicate the recorded time series making the selection of interval arrival times a difficult task. Two examples of test environments which result in source wavelet multiples are remediation sites which contain concrete or stone columns and stratigraphic profiles which contain significant impedances between layering resulting in seismic source wavelet reflections.

As previously stated, the source wavelet multiples result in more complicated seismic time series. The recorded output is mathematically represented as the convolution of the source wavelet with the direct primary wavelet and the reflection coefficients between the different mediums present. The reflection coefficient for a normal incident wavelet is given as:

$$R = \frac{(\rho_2 V_2 - \rho_1 V_1)}{(\rho_2 V_2 + \rho_1 V_1)} \quad (1)$$

where R is defined as the reflection coefficient, ρ is the medium density and V is the medium velocity and it is assumed that the source wavelet travels from medium 1 and is reflected at medium 2. The mathematical representation of the convolution model is represented as follows:

$$z(k) = \sum_{i=1}^{k} \mu(i)\, S(k-i) + v(k), \; k = 1, 2, \cdots, N \quad (2)$$

where $z(k)$ is the measurement, $\mu(i)$ is the reflectivity sequence, $S(i)$, i = 0, 1, ··· is a sequence associated with the seismic source wavelet, and $v(k)$ is the measurement noise. This paper outlines a seismic cone deconvolution algorithm where reflection coefficients are extracted from the raw seismic time series so that interval arrival times are more easily obtained for source wavelet multiples. In addition, when only a direct source wavelet is present in the recorded time series, seismic deconvolution can simplify and automate the determination of the source wavelet arrival times.

2 SEISMIC CONE DECONVOLUTION KALMAN FILTER

The Kalman Filter is an optimal unbiased minimum variance recursive filter which is based on state-space, time-domain formulations of physical problems. Application of this filter requires that the physical problem be modified by a set of first order differential equations which, with initial conditions, uniquely define the system behaviour. The filter utilizes knowledge of system and measurement dynamics, assumed statistics of system noises and measurement errors and statistical information about the initial conditions. Figure 1 illustrates the essential relation between the system, the measurements and the Kalman Filter.

Figure 1 indicates the scope of information the KF takes into account. As can be seen, the statistics of the measurement and state errors are essential components of the filter. The *a priori* information provides for optimal use of any number, combination and sequence of external measurements. The KF can be applied to problems with linear time-varying systems and with non-stationary system and measurement statistics. Problems with nonlinearities can be handled by linearizing the system and measurement equations or by implementing particle filtering. The Kalman Filter is readily applied to estimation, smoothing and prediction.

Mendel (1983) has carried out extensive work in fitting geophysical problems into state-space representations for the purpose of seismic deconvolution. By formulating the seismic cone deconvolution problem into a state-space representation allows for time variance of both the seismic source wavelet and ambient background noise, and modeling assumptions such as a minimum phase source wavelet are avoided. In addition, the KF has proven to be very robust in its ability to handle approximations to the source wavelet and perform well in high noise environments.

2.1 *Standard Kalman Filter Governing Equations*

In general terms, the Kalman Filter is a method for estimating a state vector $\underline{x}$ from measurement $\underline{z}$. The state vector may be corrupted by a noise vector $\underline{w}$ and the measurement vector is corrupted by a noise vector $\underline{v}$. The filter is applicable for systems that can be described by a first order differential equation in $\underline{x}$ and a linear (matrix) equation in $\underline{z}$. The filter can be described in both continuous and discrete form. The continuous state and measurement equations are given by eqs. (3) and (4) as follows:

$$\dot{\underline{x}}(t) = F(t)\underline{x}(t) + G(t)\underline{w}(t) \quad (3)$$

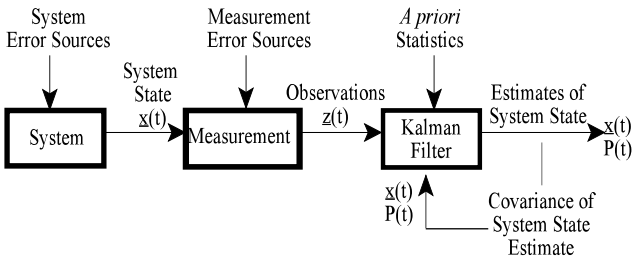

Figure 1. Block diagram of system, measurement, and Kalman Filter.

$$\underline{z}(t) = H(t)\,\underline{x}(t) + \underline{v}(t) \quad (4)$$

where $\underline{x}$ is an n-vector, $\underline{w}$ is a p-vector, and $\underline{z}$ and $\underline{v}$ are m-vectors. The random (vector) processes $\underline{w}$ and $\underline{v}$ are assumed to be zero mean, white noise processes. It is further assumed that $\underline{w}$ and $\underline{v}$ are statistically independent of each other. The corresponding discrete state and measurement equations are given by

$$\underline{x}_k = \Phi_{k-1}\underline{x}_{k-1} + \Gamma_{k-1}\underline{w}_{k-1}, \quad \underline{w}_k \approx N(\underline{0}, Q_k) \tag{5}$$

$$\underline{z}_k = H_k\underline{x}_k + \underline{v}_k, \quad \underline{v}_k \approx N(\underline{0}, R_k) \tag{6}$$

In eqs. (5) and (6), symbol *N* denotes a normal distribution with mean $\underline{0}$ and variance Q_k and R_k, respectively. In addition, Φ is defined as the *State Transition Matrix*, Γ is the *Input Transition Matrix*, and H is the *Measurement Matrix*. The discrete Kalman Filter estimation equations are outlined as follows:

State Estimate Extrapolation:

$$\hat{\underline{x}}_k(-) = \Phi_{k-1}\hat{\underline{x}}_{k-1}(+) \tag{7}$$

Error Covariance Extrapolation:

$$P_k(-) = \Phi_{k-1}P_{k-1}(+)\Phi_{k-1}^T + \Gamma_{k-1}Q_{k-1}\Gamma_{k-1} \tag{8}$$

The term $\Gamma_{k-1}Q_{k-1}\Gamma_{k-1}$ in eq. (8) is referred to as the *Noise Covariance Matrix* .

State Estimate Update:

$$\hat{\underline{x}}_k(+) = \hat{\underline{x}}_k(-) + K_k\left[\underline{z}_k - H_k\hat{\underline{x}}_k(-)\right] \tag{9}$$

Error Covariance Update:

$$P_k(+) = \left[I - K_kH_k\right]P_k(-) \tag{10}$$

I is the identity matrix in eq. (10).

Kalman Gain Matrix:

$$K_k = P_k(-)H_k^T\left[H_kP_k(-)H_k^T + R_k\right]^{-1} \tag{11}$$

Initial Conditions:

$$\mathrm{E}\left[\underline{x}_0\right] = \hat{\underline{x}}_0, \quad \mathrm{E}\left[(\underline{x}_0 - \hat{\underline{x}}_0)(\underline{x}_0 - \hat{\underline{x}}_0)^T\right] = P_0 \tag{12}$$

The computational sequence for the discrete Kalman Filter is outlined as follows:

A. At time index $k = 0$, specify initial conditions $\hat{\underline{x}}_0$, and P_0, and compute Φ_0 and Q_0.
B. At time index k=1, compute $\hat{\underline{x}}_1(-)$, $P_1(-)$, H_1, R_1, and the gain matrix K_1.
C. Using the measurement $\underline{z}_1$ at time index $k=1$, the best estimate of the state at $k=1$ is given by

$$\hat{x}_1(+) = \hat{x}_1(-) + K_1\left[z_1 - H_1\hat{x}_1(-)\right]$$

D. Update the error covariance matrix $P_1(+)$.
E. At time index $k=2$, a new measurement $\underline{z}_2$ is obtained and the computational cycle is repeated.

Smoothing is an off-line data processing procedure that uses all measurements between *0* and *T* to estimate a state at a time *t* where $0 \le t \le T$ (Gelb 1978). The smoothed estimate of $\underline{x}(t)$ based on all the measurements between *0* and *T* is identified as $\hat{\underline{x}}(t|T)$. There are three types of Kalman Filter smoothers which are identified as follows:

Fixed-interval smoothing: the time interval of measurements (i.e., the data span) is fixed, and we seek optimal estimates at some, or perhaps all, interior points.

Fixed-point smoothing: an estimate at a single fixed point in time is obtained, and the data span time T is assumed to increase indefinitely.

Fixed-lag smoothing: it is again assumed that *T* increases indefinitely, but in this case we are interested in an optimal estimate of the state at a fixed length of time in the past (i.e., $\hat{\underline{x}}(T-\delta|T)$ with δ held fixed).

In this paper we are interested in the implementation of a Fixed-Interval Smoother for seismic cone deconvolution. Mendel (1983) defines the discrete optimal fixed-interval smoothed estimate $\hat{\underline{x}}(k|N)$ (where $N = T/\Delta$ and Δ is the sampling rate) as follows:

$$\hat{\underline{x}}(k|N) = \hat{\underline{x}}_k(-) + P_k(-)\underline{r}(k|N) \tag{13}$$

where $k = N-1, N-2, \cdots, 1,$ and $n \times 1$ vector $\underline{r}$ satisfies the backward-recursive equation

$$\underline{r}(j|N) = \Phi_{j+1}^{p\prime}\,\underline{r}(j+1|N) + H_j'\left[H_jP_j(-)H_j' + R_j\right]^{-1}\left[\underline{z}_j - H_j\hat{\underline{x}}_j(-)\right] \tag{14}$$

where $j = N, N-1, \cdots, 1$ and $\underline{r}(N+1 \mid N) = 0$. In eq. (14), matrix Φ^p is defined as

$$\Phi_{k+1}^p = \Phi_{k+1}\left[I - K_kH_k\right] \tag{15}$$

The smoothing error covariance matrix $P(k \mid N)$ is defined as follows:

$$P(k|N) = P_k(-) - P_k(-)S(k|N)P_k(-) \quad (16)$$

where $k = N-1, N-2, \cdots, 1$, and $n \times n$ matrix $S(j \mid N)$, the covariance matrix of $\underline{r}(j \mid N)$, satisfies the following backward-recursive equation:

$$S(j|N) = \Phi_{j+1}^{p'} S(j+1|N)\Phi_p(j+1,j) + H_j'[H_j P_j(-)H_j' + R_j]^{-1} H_j \quad (17)$$

where $j = N, N-1, \cdots, 1$ and $S(N+1 \mid N) = 0$.

The computational sequence for the discrete fixed-interval Kalman Filter smoother can be thought of as a two pass process. In the first pass optimal real-time state estimates are obtained by implementation of previously outlines steps A to E. In the second pass results from the first-pass estimates (i.e., $\hat{\underline{x}}$ *and* P) are reprocessed starting from time index N and utilizing eqs. (13) to (17).

2.2 *Seismic Cone Deconvolution (SCD) Governing Equations*

The seismic convolution model outlined in eq. (2) may be represented as an autoregressive moving average process (ARMA) (Mendel(1983)). The ARMA model is a combination of both an autoregressive (AR) process and a moving average (MA) process. An AR time series process is generated by a linear combination of past observations plus a Gaussian random variable. The MA process is generated by a finite linear combination of past and present inputs only. In the SCD algorithm the recorded source wavelet and any possible multiples are modeled as an ARMA process which is driven by a forcing function defined as the in-situ direct wavelet and reflection coefficients.

The first step in the SCD analysis is for the user to specify the order of the ARMA process. For example, the Z transform for a fourth order ARMA model is outlined as follows:

$$V(z) = \frac{b_1 z^4 + b_2 z^3 + b_3 z^2 + b_4 z^1}{z^4 + a_1 z^3 + a_2 z^2 + a_3 z^1 + a_4} = \frac{X(z)}{U(z)} \quad (18)$$

where the parameters b_1, b_2, b_3, and b_4 define the MA process coefficients, while the parameters a_1, a_2, a_3, and a_4 define the AR process coefficients. $X(z)$ is the Z transform of the seismic time series recorded and $U(z)$ is the Z transform of the direct wavelet and in-situ reflection coefficients.

In eq. (18), the output x_{k+4} is estimated on the basis of x_{k+3} x_{k+2}, x_{k+1}, x_k, μ_{k+4}, μ_{k+3}, μ_{k+2}, and μ_{k+1} according to the following equation:

$$x_{k+4} + a_1 x_{k+3} + a_2 x_{k+2} + a_3 x_{k+1} + a_4 x_k = b_1 \mu_{k+4} + b_2 \mu_{k+3} + b_3 \mu_{k+2} + b_4 \mu_{k+1} \quad (19)$$

The SCD state-space formulation is based upon the technique utilized by Mendel (1983). Variable $y1_{k+1}$ whose Z transform is $Y1(z)$ is introduced into eq. (18) resulting in the following expression:

$$V(z) = \frac{b_1 z^4 + b_2 z^3 + b_3 z^2 + b_4 z^1}{z^4 + a_1 z^3 + a_2 z^2 + a_3 z^1 + a_4} \frac{Y1(z)}{Y1(z)} = \frac{X(z)}{U(z)} \quad (20)$$

Equation numerator and denominator terms in eq. (20) gives the following two expressions:

$$x_k = b_1 y1_{k+4} + b_2 y1_{k+3} + b_3 y1_{k+2} + b_4 y1_{k+1} \quad (21a)$$

$$\mu_k = y1_{k+4} + a_1 y1_{k+3} + a_2 y1_{k+2} + a_3 y1_{k+1} + a_4 y1_k \quad (21b)$$

By choosing $x1_k = y1_k$, $x2_k = y1_{k+1}$, $x3_k = y1_{k+2}$, and $x4_k = y1_{k+3}$ we can fit eqs. (21a) and (21b) into a state-space formulation as follows:

$$\begin{bmatrix} x1_{k+1} \\ x2_{k+1} \\ x3_{k+1} \\ x4_{k+1} \end{bmatrix} = \begin{bmatrix} 0 & 1 & 0 & 0 \\ 0 & 0 & 1 & 0 \\ 0 & 0 & 0 & 1 \\ -a_4 & -a_3 & -a_2 & -a_1 \end{bmatrix} \begin{bmatrix} x1_k \\ x2_k \\ x3_k \\ x4_k \end{bmatrix} + \begin{bmatrix} 0 \\ 0 \\ 0 \\ 1 \end{bmatrix} \mu_k \quad (22)$$

where the direct source wavelet and reflection coefficients μ_k are defined as $E[\mu_k \mu_\tau] = Q_k \delta(k-\tau) \cdot \mu_k$ is a Gaussian white noise processes with mean zero and time-variant variance of Q_k.

The discrete measurement equation is given as

$$z_k = \begin{bmatrix} b_4 & b_3 & b_2 & b_1 \end{bmatrix} \begin{bmatrix} x1_k \\ x2_k \\ x3_k \\ x4_k \end{bmatrix} \quad (23)$$

The computational sequence for the discrete SCD is outlined as follows:

F. Specify order of the convolution ARMA process and derive coefficients (e.g., a_1, a_2, a_3, a_4, b_1, b_2, b_3,

and b_4 - subsequently addressed in this paper).
G. Define state-space matrix equation (i.e., eq. (22)) and measurement equation (i.e., eq. (23)).
H. Obtained estimates of the filtered states (i.e., $\hat{\underline{x}}$) by implementing previously outlined Kalman Filter steps A to E.
I. Obtained smoothed estimates (i.e., eqs. (13) and (14)) by utilizing the values derived for $\hat{\underline{x}}$ *and* P in step H and utilizing eqs. (13) to (17).
J. Derive reflection coefficients by implementing (Mendel (1983)):

$$\hat{\mu}(k|N) = Q(k)\,\Gamma'\,r(k+1|N) \tag{24}$$

The state-space formulation outlined in eq. (22) could also be modified to accommodate a more complicated ambient noise process as opposed to the assumed white measurement noise (Baziw and Weir-Jones (2002)). For example, a Gauss-Markov process can be used to describe many physical phenomena and is a good candidate to model possible seismic cone ambient measurement noise.

The Gauss-Markov process has a relatively simple mathematical description. As in the case of all stationary Gaussian processes, specification of the process autocorrelation completely defines the process. The variance, σ^2, and time constant, T_c (ie., $\beta = 1/T_c$), define the first-order Gauss-Markov process. The SCD state-space formulation is simply augmented with the discrete formulation of the Gauss-Markov process so that more structure is provided to the measurement noise.

2.3 *Estimating the ARMA Parameters for a Seismic Cone Source Wavelet*

As previously stated, the first step in the SCD algorithm is for the user to determine the order of the ARMA process and subsequently derive the necessary model parameters. This portion of the SCD analysis is referred to as *system identification*. The maximum-likelihood of approximating the true source wavelet with an ARMA model increases monotonically with increasing system order, while the computational cost of increasing the system order is proportional to n^3 where n is the ARMA model order (Mendel 1983). In general terms, the process of determining the ARMA model order is a trial and error approach. In this analysis, the investigator chooses a model which has the smallest number of parameters while meeting a performance index requirement that measures how well the ARMA model fits the actual in-situ model.

The technique utilized by the author in deriving the ARMA model parameters is based upon the work of Ogata (1987). In this approach to *system identification*, a least squares cost function which is defined as the difference between the ARMA model response and the corresponding experimental response is minimized.

2.3.1 *ARMA Parameter Estimation by the Least Squares Method*

The derivation of the ARMA model parameters by utilizing a least squares method is demonstrated by again considering the 4th order (i.e., $n = 4$) ARMA model given in eq. (18). If the numerator and denominator of eq. (18) is multiplied by z^{-4}, we obtain

$$\frac{X(z)}{U(z)} = \frac{b_1 + b_2 z^{-1} + b_3 z^{-2} + b_4 z^{-3}}{1 + a_1 z^{-1} + a_2 z^{-2} + a_3 z^{-3} + a_4 z^{-4}} \tag{25}$$

In eq. (25), the output x_k is estimated on the basis of x_{k-1} x_{k-2}, x_{k-3}, x_{k-4}, μ_k, μ_{k-1}, μ_{k-2}, and μ_{k-3} according to the following equation:

$$\hat{x}_k = -a_1 x_{k-1} - a_2 x_{k-2} - a_3 x_{k-3} - a_4 x_{k-4} + b_1 \mu_k + b_2 \mu_{k-1} + b_3 \mu_{k-2} + b_4 \mu_{k-3} \tag{26}$$

where $\hat{x}_k$ is the estimated value of $\underline{x}_k$.

The error between the estimated output value and actual output value is defined as follows:

$$\varepsilon_k = x_k - \hat{x}_k \tag{27}$$

Since x_k depends on past data up to n sampling periods earlier, the error ϵ_k is defined only for $k \geq n$. By substituting eq. (26) and $k = n, n+1, \cdots N$ into eq. (27) and combining the resulting $N–n+1$ equations into vector-matrix equation, we obtain:

$$\underline{x}_N = C_N \underline{q}_N + \underline{\varepsilon}_N \tag{28}$$

where $\underline{x}_N = [x_4\, x_5 \cdots x_N]$, $\underline{q}_N = [-a_1, -a_2, -a_3, -a_4, b_1, b_2, b_3, b_4]$, $\underline{\varepsilon}_N = [\varepsilon_4\, \varepsilon_5 \cdots \varepsilon_N]$, and C_N is defined as:

$$\left[\begin{array}{cccc|cccc} x_3 & x_2 & x_1 & x_0 & \mu_4 & \mu_3 & \mu_2 & \mu_1 \\ x_4 & x_3 & x_2 & x_1 & \mu_5 & \mu_4 & \mu_3 & \mu_2 \\ . & . & . & . & . & . & . & . \\ . & . & . & . & . & . & . & . \\ . & . & . & . & . & . & . & . \\ x_{N-1} & x_{N-2} & x_{N-3} & x_{N-4} & \mu_N & \mu_{N-1} & \mu_{N-2} & \mu_{N-3} \end{array}\right]$$

The least squares performance index is defined as:

$$J_N = \frac{1}{2}\sum_{k=4}^{N} \varepsilon_k^2 = \frac{1}{2}\underline{\varepsilon}_N^t \underline{\varepsilon}_N \tag{29}$$

The least squares method involves minimizing eq. (29) such that the ARMA parameter values will best fit the observed data. In Ogata's formulation it is assumed that the input sequence $\{\mu_k\}$ is such that for $N>4$, $C_N^t C_N$ is nonsingular. Ogata shows that the optimal estimate of $\hat{\underline{q}}_N$ is defined as:

$$\hat{\underline{q}}_N = \left[C_N^t C_N\right]^{-1} C_N^t \underline{y}_N \tag{30}$$

In eq. (30) it is required that $\{\mu_k\}$ is sufficiently time-varying so that $C_N^t C_N$ is nonsingular.

Equation (30) is a first best estimate (in a least squares sense) of the ARMA parameters. Ogata presents a subsequent recursive formulation for the estimate of ARMA parameters utilizing eq. (30) as an initial estimate. The recursive least square estimation is defined as

$$\hat{\underline{q}}_{N+1} = \hat{\underline{q}}_N + K_{N+1}\left[y_{N+1} - \underline{c}_{N+1}\hat{\underline{x}}_N\right] \tag{31}$$

where

$$K_{N+1} = \frac{\left[C_N^t C_N\right]^{-1}\underline{c}_{N+1}^t}{1 + c_{N+1}\left[C_N^t C_N\right]^{-1}\underline{c}_{N+1}^t}$$

and

$$\underline{c}_{N+1} = \left[y_N \vdots y_{N-1} \vdots y_{N-2} \vdots y_{N-3} \vdots \mu_{N+1} \vdots \mu_N \vdots \mu_{N-1} \vdots \mu_{N-2}\right]$$

The method utilized by the author for determining the ARMA parameters for the source wavelet is to first convolve the isolated wavelet with a highly variable and known white noise process with mean zero and unity variance. This insures that $\{\mu_k\}$ is sufficiently time-varying so that $C_N^t C_N$ is nonsingular. Initial estimates of the ARMA parameters are obtained by implementation of eq. (30), known $\{\mu_k\}$, and the convolved output sequence $\{y_k\}$. The initial estimates of $\hat{\underline{q}}_N$ are then feed into the recursive estimation equation defined by eq. (31) until the performance index (eq. (29)) reaches a predefined minimum.

3 EVALUATING THE SCD ALGORITHM WITH SIMULATED FINITE DIFFERENCE DATA

This section presents test bed simulation results when implementing the optimal estimation algorithm previously outlined. The first step in the simulation was to define a seismic source wavelet. Amini and Howie (2003) utilized a finite difference program (FLAC) to model the in-situ seismic cone wavelets. Figure 2 illustrates the simulated source wavelet generated by Amini and Howie (2003) obtained by personal communication. SCPT has the very beneficial feature in that the SH source wavelet is highly repeatable from site to site and its basic form is consistent through out a seismic profile except for the reduction in amplitude due to geometric spreading. The wavelet shown in Fig. 2 was generated by assuming a uniform halfspace with an in-situ shear wave velocity of 180 m/s and a sampling rate of 0.02 ms.

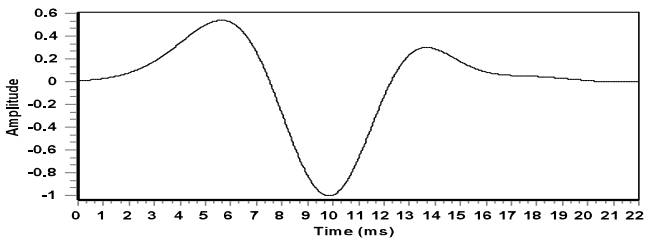

Figure 2. Finite difference simulate source wavelet.

The algorithm outlined in Section 2.3.1 was then implemented on the data illustrated in Fig. 2. In deriving the necessary ARMA parameters a 5th order AR and MA were utilized with a data compression ratio of 16 to 1 so that the sampling rate became 0.32 ms. In addition, it was found that ARMA model estimation algorithm worked best when the source wavelet was time reversed. The only impact that time reversing the source wavelet has on the SCD algorithm is that the recorded seismic time series must be time reversed when processing. Figure 3 illustrates the results of the ARMA estimation of the time reversed source wavelet shown in Fig. 2.

The estimated ARMA model is then convolved with the impedance structure illustrated in Fig. 4 to give the output shown in Fig. 5.

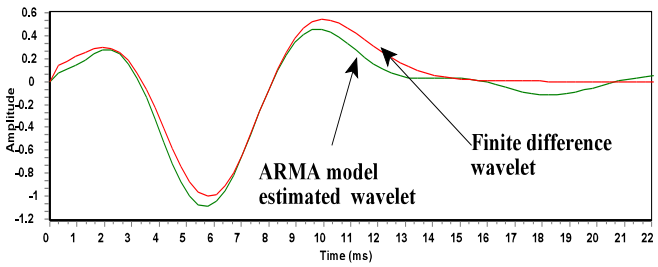

Figure 3. Estimating source wavelet in Fig. 2 with 5th order ARMA model

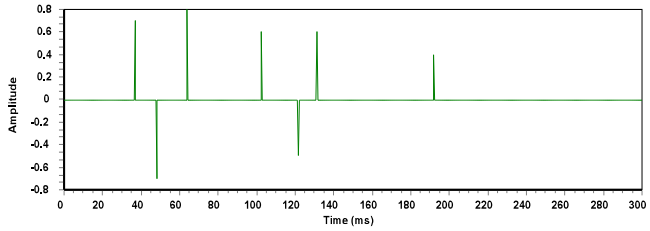

Figure 4. Reflection coefficients utilized to test the performance of the SCD algorithm.

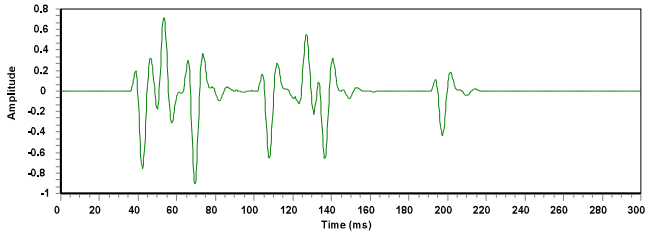

Figure 5. Output after convolving ARMA wavelet with reflection coefficients shown in Fig. 4.

If the SCD algorithm outlined in Section 2.2 is applied to the seismic data shown in Fig. 5, the reflection coefficients illustrated in Fig. 4 are recovered exactly.

Gauss-Markov noise is then added to the seismic data shown in Fig. 5 where a time constant of T_c = *0.02 ms* and standard deviation of σ = *0.002* were specified. The SCD algorithm derived the output shown in Fig. 6. As is illustrated in Fig. 6 the arrival time location of the reflection coefficients is recovered exactly but there is some degradation in the estimation of the amplitudes. The SCD algorithm gives accurate estimates of the relative amplitudes of reflection coefficients.

The SCD algorithm was next tested for its ability to derive the reflection coefficients within a high noise environment. Figure 7 shows the seismic data of Fig. 5 with Gauss-Markov noise of T_c = *0.02 ms* and σ = *0.08* added.

The SCD algorithm derived the estimates illustrated in Fig 8. As is shown in Fig. 8, the arrival time location of the reflection coefficients is recovered exactly but the algorithm fails to determine the amplitudes. The SCD algorithm gives accurate estimates of the relative amplitudes of the reflection coefficients which facilitates the investigator to recover the true amplitudes.

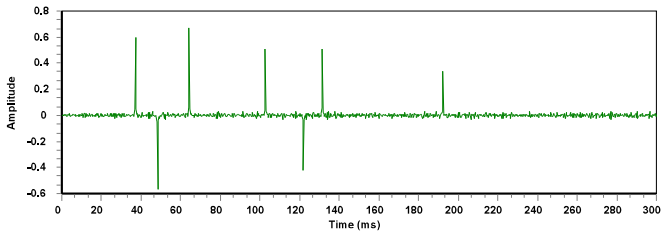

Figure 6. SCD estimated reflection coefficients.

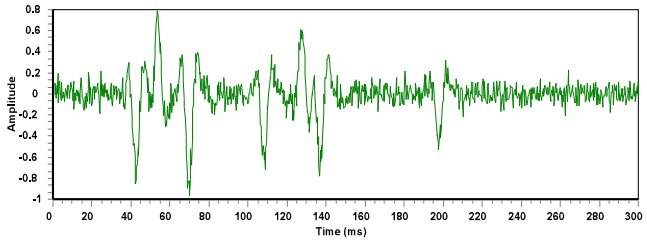

Figure 7. Seismic data of Fig. 5 with Gauss-Markov noise of T_c = 0.02 ms and σ = 0.08 added.

Figure 9 shows the SCD output for the data derived when the true time reversed wavelet of Fig. 2 is convolved with the reflection coefficients in Fig. 4 and Gauss-Markov noise of T_c = *0.02 ms* and σ = *0.08* is added. The SCD algorithm provided very similar results to those illustrated in Fig. 8.

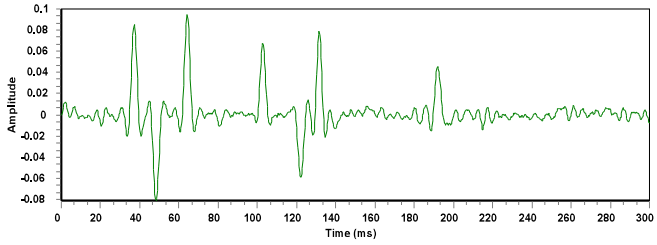

Figure 8. SCD estimated reflection coefficients for data shown in Fig. 7.

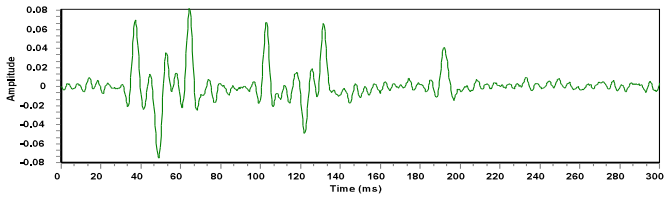

Figure 9. SCD estimated reflection coefficients when the source wavelet illustrated in Fig. 2 is utilized.

The SCD algorithm was next tested for its ability to extract the primary wavelet and the reflection coefficients when only a portion of the source wavelet is modeled. Figure 10 shows a 4th order AR and MA

approximation to the portion of the time reversed source wavelet shown in Fig. 2. In this case the data was compressed at a 4 to 1 ratio resulting in a *0.08 ms* sampling rate.

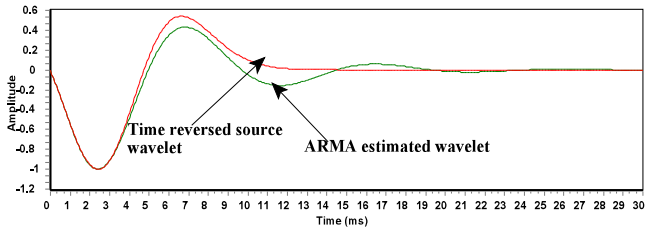

Figure 10. 4th order ARMA approximation to portion of source wavelet shown in Fig. 2.

Figure 11 illustrates the SCD estimated reflection coefficients from the data shown in Fig. 7 (true time reversed wavelet utilized) and when only a portion of the time reversed source wavelet was modeled as illustrated in Fig. 10. As is shown in Figure 11 the SCD algorithm recovered the exact time location (time shifted by constant amount due to truncated wavelet approximation) when only a portion of the source wavelet was modeled.

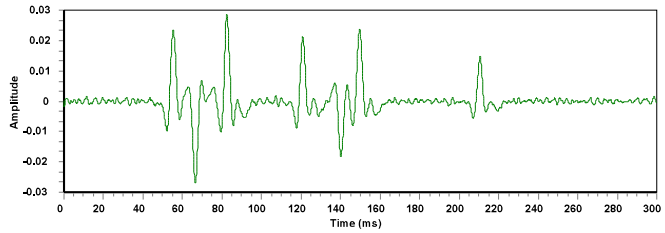

Figure 11. Estimated reflection coefficients when 4th order ARMA model utilized.

Figure 12 illustrates the ability of the SCD algorithm to simplify and automate the determination of the source wavelet arrival times when only a primary wavelet is present.

4 CONCLUSIONS

In SCPT there are site conditions which may result in source wavelet multiples. These multiples complicate the recorded time series making the selection of interval arrival times a difficult task. This paper outlined a state-space smoothing Kalman Filter algorithm which deconvolves impedance structures from source wavelets by modeling the convolution process as an ARMA model. The ability to obtain the in-situ reflection coefficients from multiples and/or reflections allows the investigator to map out under ground structures.

The SCD algorithm was demonstrated to be highly robust and accurate when utilizing approximations to the source wavelet and in high noise environments. In addition, when only a direct source wavelet is present in the recorded time series, the SCD algorithm significantly simplified and automated the determination of the source wavelet arrival times.

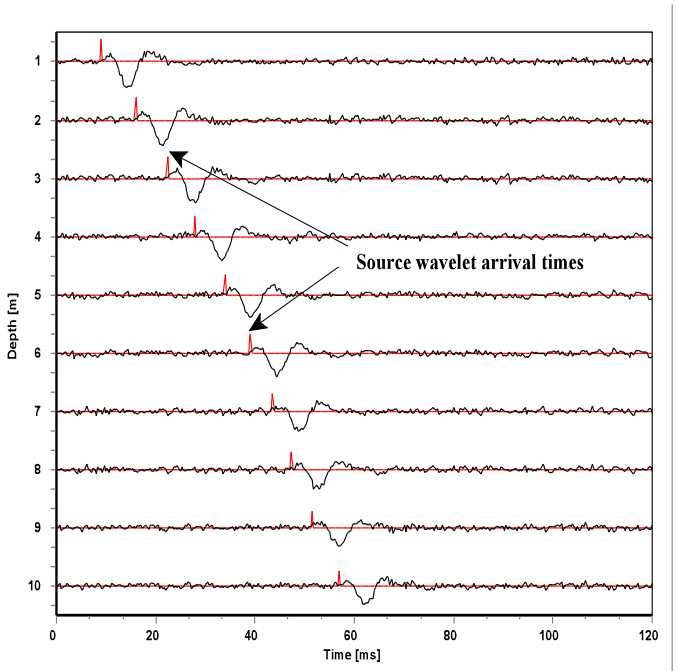

Figure 12. Estimating source wavelet arrival times from vertical seismic profile using SCD algorithm.

REFERENCES

Amini, A. and Howie, J.A. 2003. Numerical simulation of downhole seismic cone signals. 56th Canadian Geotechnical Conference, Winnipeg, Manitoba, Canada, September 28 to October 1, 2003.

Andrus, R.D., Stokoe, K.H. and Chung, R.M. 1999. Draft guidelines for evaluating liquefaction resistance using shear wave velocity measurements and simplified procedures, NISTIR 6277.National Institute of Standards and Technology, Gaithersburg, Md.

Baziw, E.J. 1993. Digital filtering techniques for interpreting seismic cone data. Journal of Geotechnical Engineering, ASCE, 119(6): 98-1018.

Baziw, E.J. 2002. Derivation of seismic cone interval velocities utilizing forward modeling and the downhill simplex method. Canadian Geotechnical Journal, 39: 1-12.

Baziw, E.J. and Weir-Jones, Iain 2002. Application of Kalman filtering techniques for microseismic event detection. Pure and Applied Geophysics, 159: 449-473.

Campanella, R.G., Robertson, FTC and Gillespie, D. 1986. Seismic cone penetration test. Proc. INSITU86. ASCE, Geot. Spec. Publ. No. 6, June: 116-130.

Finn, W.D. L. 1984. Dynamic response analysis of soils in engineering practice. *In* Mechanics of engineering materials. John Wiley & Sons Ltd., New York. Chapter 13.

Gelb, A. 1978. Applied optimal estimation. 4th Edition, MIT Press, Cambridge, Mass.

Mendel, J.M. 1983. Optimal seismic deconvolution an estimation-based approach. 1st ed., Academic Press.

Ogata, J. 1987. Discrete process control. 1st ed., Prentice- Hall, New Jersey. pp. 856-867.